

OPTIMIZATION APPROACHES FOR THE SHEAR-POSTBUCKLING DESIGN OF THERMOPLASTIC THIN-PLY COMPOSITE SHELLS IN HELICOPTERS

Michael Mauersberger[1], Joanna Rehfeldt[1], Falk Hähnel[1], Johannes Markmiller[1]

[1]Dresden University of Technology (TUD), Institute of Aerospace Engineering,
Chair of Aircraft Engineering, 01062 Dresden, Germany

Abstract

There is a need to apply innovative approaches for the design of helicopter structures to reach sustainability goals while maintaining structural efficiency. Thermoplastic high-performance carbon fibre-reinforced plastics (CFRP) enable load-oriented material properties with low density while offering energy-effective production and benefits in recycling at the same time. Moreover, thin-ply CFRP help to push design limits of laminated structures beyond present limits regarding quasi-isotropic or damage-tolerant laminates with better structural quality and lower mass.

The present study proposes a stepwise approach for the design of stiffened shell structures. The skin layup and stringer configurations were optimized separately in design levels 1 and 2 to reduce the overall computational effort. Simple line stringer models in design level 2 featured generic properties which were transferred to concrete stringer cross-sections in design level 3. Several optimization function formulations were analysed to generate structural solutions with distinctive performance. This was achieved more effectively for structures with additional stringers in design level 2. Optimizing the buckling factor incorporated large variations over a narrow range of structural solutions. A different objective is suggested, e.g., maximizing the failure load instead, to yield robust solutions over an extended domain. However, with high values for the buckling factor even for detailed models in design level 3, the viability of the present postbuckling design approach is confirmed. Stringer tails close to skin buckles were identified as the most critically stressed structural parts. Aluminium reference structures could not reach the structural performance of its thermoplastic CFRP counterpart, not even for quasiisotropic layups.

Limitations regarding the transfer of simple structural solutions in design level 2 to more detailed models in design level 3 should be counteracted in future investigations, e.g., by formulating additional optimization constraints. Moreover, non-linear material models including plasticity and damage mechanisms should be included in advanced studies for a more reliable failure prediction.

Keywords: structural optimization, shear-postbuckling, thermoplastic thin-ply composites, helicopters

1. Introduction

The design of helicopter structures requires novel, innovative approaches for achieving sustainability goals while maintaining structural integrity and efficiency. First, high-performance carbon fibre-reinforced plastics (CFRP) facilitate load-oriented material properties with low density [1]. Especially thermoplastic matrix composites offer energy-effective production methods such as ultrasonic welding [2] or in situ consolidation [3,4]. At the same time, these methods accompany advanced automation possibilities resulting in higher scalability and lower production costs [5]. Thermoplastic CFRP are furthermore advantageous compared to thermoset materials in terms of environmental sustainability due to energy-efficient storage and recycling capabilities [5].

Second, design limits of CFRP laminated structures can be extended by a considerably reduced ply thickness in so called thin-ply composites [6]. With thicknesses below 0.1, up to 0.02 millimetre [6,7], design approaches like quasi-isotropic (QI) or damage-tolerant laminates can reach higher structural

quality. Moreover, the in-situ properties, i.e. properties within the laminate, increase in terms of tensile strength [8], compressive strength [7], elastic modulus [9], and delamination resistance [10,11]. Consequently, structural mass may be reduced and lower energy demand in the aircraft operation phase [12] effectively contributes to sustainability goals. This approach was recently used by large helicopter manufacturers such as Airbus Helicopters and plays an important role in future design considerations [13]

1.1 Shear-postbuckling of helicopter structures

Further mass savings can be realized by permitting structural responses within the postbuckling regime. Conservative designs for stiffened shell structures in aircraft only allow local buckling above design limit load. With the design ultimate load commonly being defined as 1.5 times limit load, this results in load ratios between failure and first buckling of no more than 1.5. This number is here defined as the buckling factor λ_B. Previous efficient designs of side shell structures in helicopters are made from aluminium with thicknesses below 1 millimetre and permit buckling below limit load. Due to the isotropic, highly ductile behaviour of aluminium, also crash load cases with buckling factors above 10 can be achieved.

This is currently not the case when using CFRP material mainly due to its rather brittle nature. There are several investigations in the past two decades dealing with the postbuckling behaviour of layered stiffened composite shells. Experimental studies by Zimmermann et al. [14], Bisagni [15], or Degenhardt et al. [16] on unoptimized composite stiffened shells suggest buckling factors in the range of 1.5 to 4.0 for compressive and shear loading. Non-linear finite element (FE) simulations with high resolution were used to validate the results [16,17]. Important aspects regarding the structural behaviour until failure are damage initiation and collapse mechanisms [14,18-21] which should also be included into design considerations for stiffened shells [22,23].

Concrete design approaches were formulated by Fink et al. [13] for thin-ply composites using QI laminates for stiffened airframe shells of a helicopter.

1.2 Structural optimization for preliminary design

In general, the computational effort of FE simulation scales with the detail level of the structural models and non-linearities. Therefore, high-quality postbuckling simulations with full damage modelling are less feasible for automatic design by means of optimization. This is why only preliminary designs may be generated [24] by using efficient methods with less details such as semi-analytical or approximation methods [16,25-28]. Due to the discrete nature of composite designs, integer programming or genetic algorithms seem to be suitable [29-31]. However, the objective of layup optimization can be formulated in a continuous way by optimizing lamination parameters and interpret the appropriate layup angles afterwards [32,33]. Especially the optimization of QI layups was investigated to resemble rather easily predictable properties in composite design [34-36]. Benefits also arise in structural certification utilizing straightforward analogies to isotropic materials, e.g., aluminium. Gradient-based optimization yielded solutions with optimal, but hardly workable ply orientation angles [36]. In contrast, gradient-free optimization methods, such as genetic algorithms, readily achieve preset angle values like the common values 0°, 90°, and ±45° [31].

Using fast, approximate methods for FE postbuckling analysis has two drawbacks: On the one hand, the analysis of shear-postbuckling is limited here to approximations or symmetric cross-ply and angle-ply laminates. On the other hand, damage is rarely considered. Faggiani et al. [24] investigated postbuckling of a stiffened shell-structure under compressive loading. Damage was modelled at the cohesive zone between stiffener and skin. Layups were optimized via genetic algorithms due to the integer nature of the design space. In order to reduce calculation effort, a global FE model was used, that forwards the postbuckling loading to a local stiffener-skin model. Damage in the stiffener-skin interface could be reduced by 42% by means of optimization. Also, Qu et al. [37] demonstrated the benefits of design via optimization. They investigated the postbuckling behaviour of a composite

wing with a similar approach of global-local modelling, but without damage consideration. Mass savings of up to 44% could be achieved.

Table 1 – Symbols and abbreviations.

symbol/abbreviation	description	unit
A	cross-sectional area	mm²
$\boldsymbol{A} = (A_{ij})$	in-plane stiffness matrix	N/mm
$\boldsymbol{B} = (B_{ij})$	coupling stiffness matrix	N
$\boldsymbol{D} = (D_{ij})$	out-of-plane stiffness matrix	Nmm
E, G	elastic modulus (Young, shear)	GPa
F_B	buckling load	N
F_f	failure load	N
$F_{\max}$	maximum force in structural analysis	N
$\boldsymbol{f} = (f_1, f_2)^T$	optimization objective functions	div.
$\boldsymbol{g} = (g_k)$	optimization constraints	div.
$I_{\eta\eta}$, I_{zz}, I_t	cross-sectional area moments	mm⁴
K_{post}	postbuckling stiffness	N/mm
K_{pre}	prebuckling stiffness	N/mm
l_x, l_y	panel side lengths	mm
Δl_{1b}, Δl_{1c}, Δl_{2b}	relative stringer offsets	–
m	structural mass	kg
n_l	number of plies	–
n_{S1}, n_{S2}	number of stringers	–
R	material strength	MPa
s	structural displacement in load direction	mm
α_S	stringer angle	° (degree)
λ_B	buckling factor	–
ν	Poisson's ratio	–
CF-LMPAEK	carbon-fibre low-melt polyaryletherketone	–
CFRP	carbon-fibre reinforced plastics	–
FE	finite element	–
MPC	multi-point constraint	–
QI	quasi-isotropic	–

1.3 Aim of this study

This study presents a methodology for the preliminary shear-postbuckling design of composite stiffened shell structures in helicopters. Thermoplastic thin-ply material serves as a basis for extended design limits. Multi-objective optimization via evolutionary algorithms and non-linear FE analysis is used to generate structural designs. In a multi-level design approach, skin layups as well as stringer layout and cross-sectional properties are optimized for a low structural mass and a favourable buckling and postbuckling response concurrently. Therefore, different objectives are investigated, such as maximum first buckling load, buckling factor, and postbuckling stiffness. The

aim is here

- to demonstrate the viability of a stepwise design approach, including direct non-linear structural analysis with failure evaluation,
- to determine how far can an optimized buckling factor exceed the common value of 1.5, and
- to quantify to which extent can thermoplastic thin-ply CFRP material exhibit better structural performance compared to established structures.

This paper is divided into seven sections: Section 2 describes the materials and methods used for this study. Section 3 covers the multi-level design approach by presenting each optimization task and the appropriate results. Last two Sections 4 and 5 discuss the final results and give an outlook for further investigations, respectively. All symbols and abbreviations used throughout this paper are summarized in Table 1.

2. Material and methods

The present study puts together multi-objective optimization as a means for the preliminary design of stiffened shell structures with low mass and favourable postbuckling properties. Therefore, the optimizer GEOpS² is used together with the non-linear FE solver b2000++pro that are both already validated in past studies [38-41]. They are part of an optimization workflow (cf. Figure 1) used for three design levels:

(1) First, laminate optimization without stiffening serves to find QI and optimized anisotropic properties of the pure composite shell structure. This approach is viable since thin-ply material offers a larger design freedom even for very low laminate thicknesses.

(2) Second, the additional optimization of stiffening positions and properties offers insights into advantageous arrangements for postbuckling design. Only coarse FE models are used in this level with line geometries for stringer stiffening to reproduce an approximate structural behaviour.

(3) In the third level, arrangements from level 2 provide a basis for a more detailed modelling of the stringer stiffening including the cohesive bonding zone to the skin. Hence, suggestions for the stringer debonding behaviour may be derived.

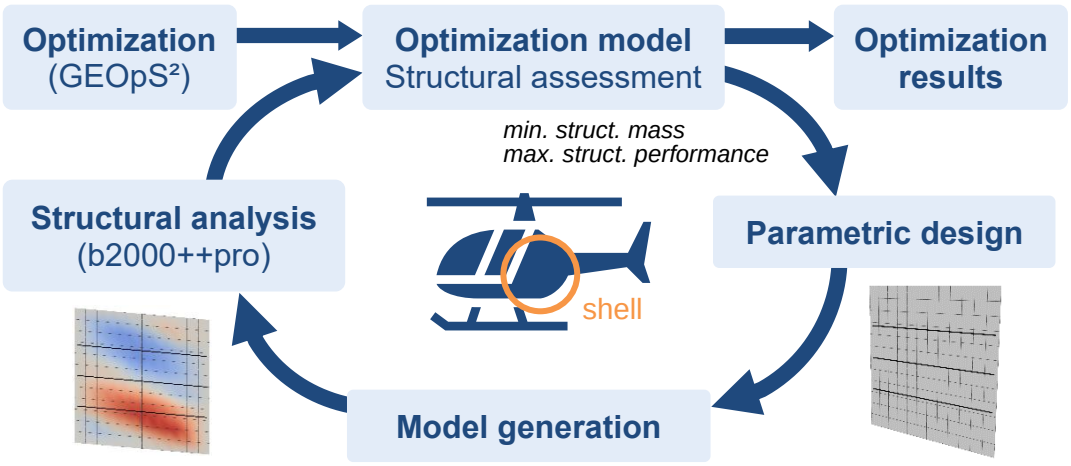


Figure 1 – Optimization workflow for the shear-postbuckling design of stiffened shell structures in helicopters.

The optimization consists of four main modules: the structural analysis, an automatic model generator, a parametric design space, and the optimization model. They are described in the following.

2.1 Model generation

This study considers a stiffened shell structure in form of a shear-loaded panel with stringers (cf. Figure 2). Quadratic dimensions of 440×440 mm² represent the typical scale for a helicopter side-

shell structure on a sub-component level. The left border with $x = 0$ is clamped while the upper right corner with $(x, y)^T = (l_x, l_y)^T$ is loaded downwards, where l_x and l_y are the panel width and height, respectively. The panel skin is modelled via 8-node shell elements with quadratic shape functions. The shear frame is modelled efficiently by means of FE constraints: The nodal z-rotation is kept free while the x- and y-rotation as well as the z-displacement is set to zero at the borders. Multi-point constraints (MPC) are set for all free borders. All nodes of the left border with $x = l_x$ follow the same y-displacement as the topmost node, which bears the loading. The nodal displacements of the upper and lower border are defined so that a straight line is ensured. An additional 2-node beam element with a penalty material stiffness of $E_{\mathrm{pen}} = 10^8$ MPa at each of these borders preserve a constant border length under deformation.

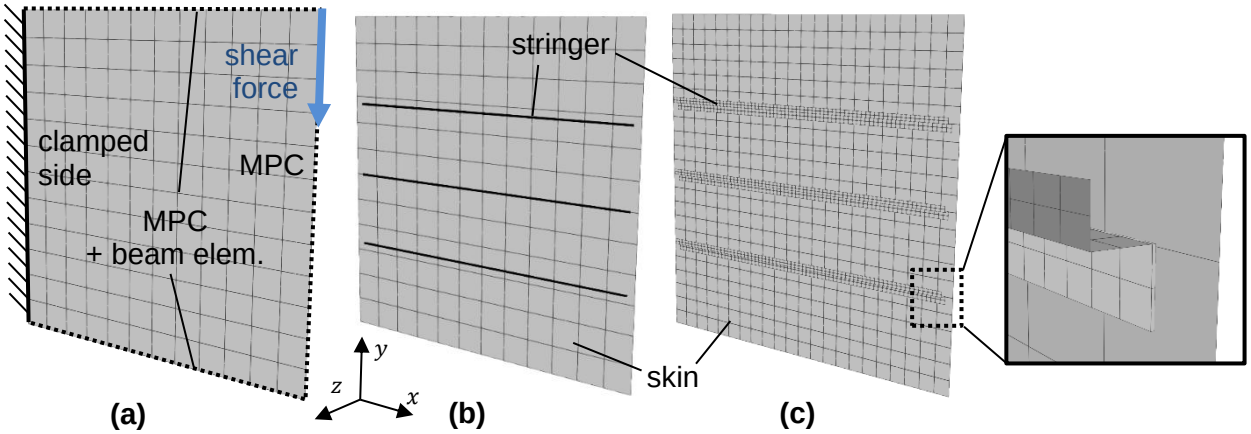


Figure 2 – Shear panel model: (a) Without stringers (design level 1), panel definition. (b) With simple stringers as lines (design level 2). (c) With detailed stringers (design level 3).

Random geometric imperfections of the nodal z-coordinate help the non-linear FE solver to find the proper bifurcation point before postbuckling. A maximum imperfection of 1 % of the skin laminate thickness is assumed here.

Stringers in design level 2 are modelled as line geometries that are meshed with 2-node beam elements with cubic shape functions. The corresponding nodes are tied to the panel by means of MPC where the nodal degrees of freedom follow the shape functions of the shell elements in terms of its quadratic shape functions.

There are differences in the modelling of design level 3 regarding a larger number of elements as well as more sophisticated stringer geometries. They are regarded as Z-stringers with shell elements along the flange, the web, and the cap. For all shell parts, a constant layup $[45/\text{-}45/0/0/0/90]_s$ with the same ply properties as of the skin is considered. A cohesive zone with the total thickness of the stringer layup is included between the flange and the skin in order to represent the stresses at the bonding interface. 20-node hexahedral volume elements with quadratic shape functions form the mesh of this zone. All nodes in the plane of the panel are tied to the skin via MPC contacts as in the coarse model of design level 2.

Table 2 summarizes the element types and lengths of all mesh parts for design levels 1 to 3.

A carbon-fibre composite with low-melt polyaryletherketone (CF-LMPAEK) matrix was chosen for analysis. Compared to composites with conventional thermoplastic matrix material such as polyetheretherketone (PEEK), CF-LMPAEK offers better workability and a broader application [42]. Material properties were defined in the present study for a unidirectional tape with 34 % resin content. A ply thickness of 43.8 µm was assumed which resembles a thin-ply material [6,7]. Pure LMPAEK properties were defined for the cohesive zone of design level 3. Aluminium material served as a reference for the comparison to previous designs of stiffened stell structures. The Hashin failure criterion for composites [43] was applied for the CF-LMPAEK, while the cohesive zone and the reference aluminium failed according to the Von-Mises equivalent stress. All material property values

are listed in Table 3. E, ν, G, R, and ρ stand for the elastic modulus, the Poisson's ratio, the shear modulus, the material strength, and the density, respectively. Indices ∥ and ⊥ represent the direction parallel and perpendicular to the fibre direction.

Table 2 – Mesh properties of the structural parts at each design level.

design level	structure	resolution	element size / mm
1	skin	12×12	36.7
2	skin	12×12	36.7
	stringer	–	20
3	skin	22×22	20
	stringer	–	6

Table 3 – Material properties used for the CF-LMPAEK composite, the pure LMPAEK matrix, and the aluminium reference. Tensile and compression strengths are denoted by "+" and "-", respectively.

material	E / GPa	ν	G / GPa	R / MPa	ρ / kg/mm³
CF-LMPAEK	∥: 135	∥⊥: 0.26	∥⊥: 4.30	∥: +2410, -1300	1.60×10^{-6}
	⊥: 10	⊥⊥: 0.30	⊥⊥: 3.85	⊥: +86, -115	
				∥⊥: 152	
				⊥⊥: 100	
LMPAEK	3.7	0.35	1.37	91	1.27×10^{-6}
aluminium	75	0.33	28.2	270	2.67×10^{-6}

2.2 Parametric design space

Variable parameters of the design configurations were specified for the optimization. Besides the layup, i.e., the number and orientation of plies in the skin laminate, stringer positions and cross-sectional properties were varied by the optimizer.

Permitted stringer positions were grouped into four configurations: (A) parallel stiffening, (B) angle stiffening, (C) parallel frames, and (D) angle frames. Configurations A and B describe parallel stringer positions parallel or with an angle to the panel sides, respectively. On the other hand, C and D stand for frames within the panel area, either parallel or with an angle to the sides. All configurations had y-symmetric stringer positions and a free margin of 10 millimetres. Design variables were defined as the number of stringers n_{S1}, n_{S2} for each stiffening and offsets Δl_{1b}, Δl_{1c}, Δl_{2b} from the border or the centre relative to the panel size or the extended diagonal. An additional stringer angle α_S was defined for configurations B and D. Figure 3 illustrates examples of stringer positions and the appropriate design variables of each configuration.

Stringer cross-sectional properties were formulated generically by means of the area moments of inertia $I_{\eta\eta}$, I_{zz}, and I_t, where the first two are the bending area moments with η as the in-plane coordinate perpendicular to the stringer direction, and the last as the torsional area moment. Permitted values were estimated based on values for the stringer laminate and various Z-stringer dimensions for flange, web, and cap (cf. Section 2.1). Assuming the most adverse cross-sectional shape, a maximum area $A_{\max}$ can be calculated for the bending area moments via

$$A_{\max,b} = \sqrt{12}\sqrt[4]{I_{\eta\eta} I_{zz}} \text{ (rectangular shape)} \tag{1}$$

and for the torsional area moment with

$$A_{\max,t} = \sqrt{2\pi I_t} \text{ (circular shape)} . \tag{2}$$

The total upper bound for the stringer cross-sectional area is consequently

$$A_{\max} = \max\left(A_{\max,b}, A_{\max,t}\right) . \tag{3}$$

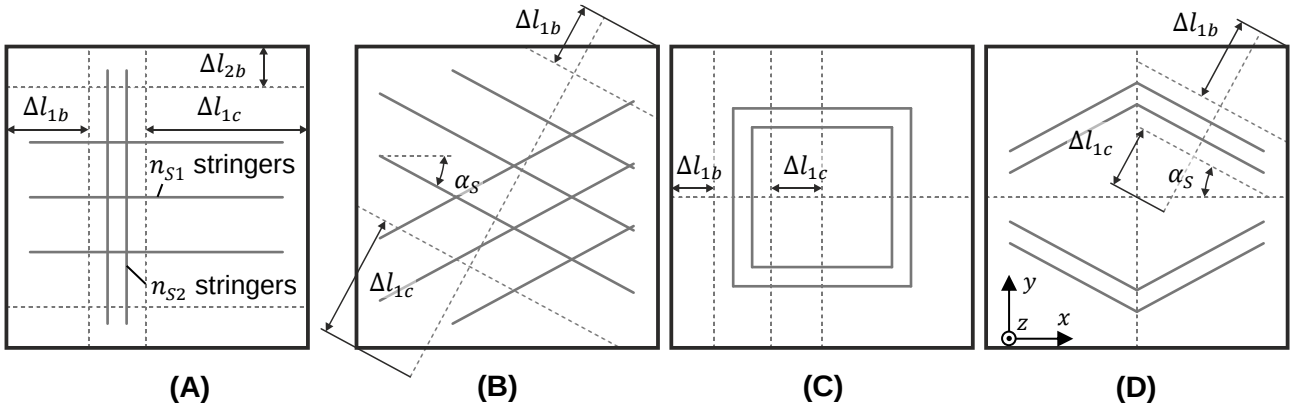


Figure 3 – Configurations of stringer positions: (A) Parallel stiffening with n_{S1} stringers in x- and n_{S2} stingers in y-direction. (B) Angle stiffening with stringer angle α_S to x-axis. (C) Parallel frames with relative offsets Δl_{1b} and Δl_{1c} for the position of equal spaced parallel stringers. (D) Angle frames.

With $A_{\max}$, the length l_S of the regarding stringer, and the material density ρ, an upper bound for the stringer mass may be estimated by means of

$$m_S = \rho\, l_S\, A_{\max} . \tag{4}$$

Constant cross-sectional properties were assumed for all stringers on one structural solution. Each design variable with the permitted domain is listed in Table 4.

Table 4 – Design variables with its permitted domain for structural optimization.

design variable	symbol	domain
number of laminate plies	n_l	$\in [1, 40]$
angle of laminate plies	α_l	$\in \{0°, 90°, 45°, -45°\}$
number of stringers	n_{S1}, n_{S2}	$\in [0, 3]$
angle of stringers	α_S	$\in [0°, 90°]$
relative offsets from the border	Δl_{1b}, Δl_{2b}	$\in [0, 1]$
relative offset from the center	Δl_{1c}	$\in [0, 1]$
bending area moment out-of-plane	$I_{\eta\eta}$	$\in [390, 1.58 \times 10^5]$
bending area moment in-plane	I_{zz}	$\in [240, 1.20 \times 10^4]$
torsional area moment	I_t	$\in [30, 700]$

2.3 Structural analysis

On the one hand, quasi-isotropy of laminate properties can be described locally without an FE analysis. It was assumed, that a QI layup requires rotational invariance for the in-plane and out-of-plane stiffnesses, expressed as the $\boldsymbol{A}$ and $\boldsymbol{D}$ matrix from the Classical Laminate Theory [44].

Therefore, the variances V_A and V_D of these values were calculated via

$$V_A = \frac{1}{n_p h_{\mathrm{lam}}} \sum_{k=1}^{n_V} \left(A_{ij,k} - \bar{A}_{ij}\right)^2 ,$$
$$V_D = \frac{1}{n_p h_{\mathrm{lam}}^3} \sum_{k=1}^{n_V} \left(D_{ij,k} - \bar{D}_{ij}\right)^2 , \tag{5}$$

with n_p as the number of probe angles of rotation, $A_{ij,k}$ and $D_{ij,k}$ as the matrix entries of $\boldsymbol{A}$ and $\boldsymbol{D}$, respectively, at the k-th probe angle of rotation, $\bar{A}_{ij}$ and $\bar{D}_{ij}$ the appropriate average values, and h_{lam} the resulting laminate thickness. Both, the variances V_A and V_D as well as the normalized sum

$$S_B = \frac{1}{h_{\mathrm{res}}^2} \sum_{ij} |B_{ij}| \tag{6}$$

of absolute $\boldsymbol{B}$ matrix entries are supposed to approach zero for ideal quasi-isotropy.

On the other hand, anisotropic laminates adjusted to specific structural performance quantities must be analysed globally, e.g., by means of an FE analysis. The shear panel model described in Section 2.1 was calculated via the non-linear FE solver b2000++pro [41]. Compared to proprietary software, it offers a fast, lightweight computation without the need for license server communication overhead. Shear-loading was simulated through state-control with a local hyperelliptic increment in the state space of load F and displacement s. The maximum simulated load F_{max} resulted from a linear precursor buckling analysis that estimated an approximated buckling and failure load, $F_{B,\mathrm{est}}$ and $F_{f,\mathrm{est}}$, via

$$F_{\mathrm{max}} = \min\left(\max\left(F_{f,\mathrm{est}}, 5\, F_{B,\mathrm{est}}\right), 40\, F_{B,\mathrm{est}}\right). \tag{7}$$

Load-displacement data from simulation was analysed to determine structural performance quantities. The curvature

$$\kappa_F(s) = \frac{\partial^2 F}{\partial s^2} \tag{8}$$

was filtered with the median of five data values each and yielded the buckling point with the state (s_B, F_B) using the first peak of κ_F greater than 50 % of the data peaks. This led directly to the prebuckling stiffness

$$K_{\mathrm{pre}} = \frac{F_B}{s_B} . \tag{9}$$

In the postbuckling regime, no constant stiffness K_{post} may be assumed so that the least value $\min\left(K_{\mathrm{post}}(s)\right)$ before material failure was used. Failure was indicated by the corresponding locally formulated criterion specified in Section 2.1. When failure occurred beyond the maximum simulated load F_{max}, the failure load F_f was extrapolated proportionally by means of the failure index. Otherwise, F_f was denoted by the simulated state with failure index equal 1. Figure 4 illustrates the analysis of the described structural performance quantities.

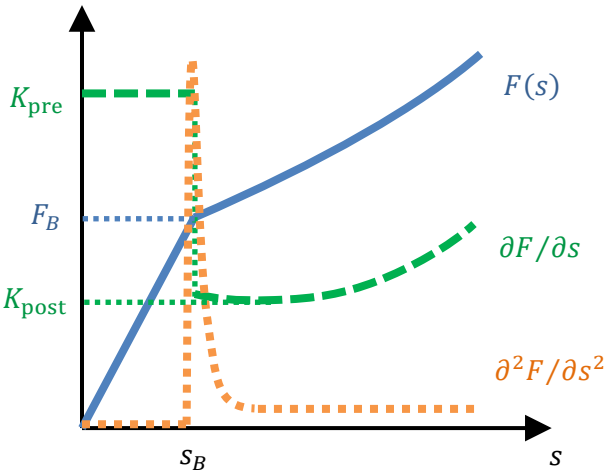


Figure 4 – Scheme of structural analysis based on the F-s history produced by non-linear analysis: Buckling point (s_B, F_B) is determined by the first large peak of the second derivative $\partial^2 F/\partial s^2$, which separates the pre- and postbuckling regime.

2.4 Optimization via evolutionary algorithms

Multi-objective optimization was carried out by means of GEOpS², a gradient-free optimizer based on evolutionary algorithms. Due to multiple objective functions, the optimized solution has the form of a Pareto set [45]. An optimization problem was posed in the form

$$\boldsymbol{f}(\boldsymbol{c}) \rightarrow \min. \;\; \text{so that} \;\; \boldsymbol{g}(\boldsymbol{c}) \leq 0 \,, \tag{10}$$

where $\boldsymbol{f} = (f_1, f_2)^T$ as the objective functions, $\boldsymbol{c}$ as the design space, and $\boldsymbol{g} = (g_k)$ as the vector of constraints. The first objective function, f_1, was set to the structural mass m, the second, f_2, to a compound quantity representing the structural performance.

In order to find an appropriate QI layup, $f_{2,QI}$ was composed of

$$f_{2,QI} = V_A + V_D + S_B \tag{11}$$

from Equations (5) and (6).

The second type of objective functions corresponds to a set of the structural performance quantities F_B, λ_B, and K_{post} that should be maximized by an anisotropic layup or the stringer configuration. A total of four objective function formulations O1 to O4 were investigated here:

$$\begin{aligned} f_{2,O1} &= w_B / F_B \,, \\ f_{2,O2} &= w_B / F_B + w_\lambda / \lambda_B \,, \\ f_{2,O3} &= w_K / K_{\mathrm{post}} \,, \\ f_{2,O4} &= w_\lambda / \lambda_B + w_B / F_B + w_K / K_{\mathrm{post}} \,. \end{aligned} \tag{12}$$

The weight factors were introduced so that each summand values had the same order of magnitude. Hence, the concrete values highly depend on the specific structural model. In the present study, they took the values $w_B = 0.005$, $w_\lambda = 30$, and $w_K = 2$.

Constraints took the form of the one-step penalty method with a quadratic penalization and the penalty factor $q = 10^8$. For the layup, no angle repetitions were allowed which led to the first constraint

$$g_1 = n_{\mathrm{rep}}\, q \tag{13}$$

with n_{rep} as the number of angle repetitions within the layup. Another constraint was introduced to produce layups that had balanced ply angles in y-direction. Although loading in only one direction was considered, this measure attenuated an overly specialization therein. All ply angles different

from 0° and 90° were summated to S_{ang} yielding the constraint

$$g_2 = S_{\mathrm{ang}}\, q\ . \tag{14}$$

Besides these constraints, laminates were designed to be symmetric.

GEOpS² involved evolutionary strategies (ES), genetic algorithms (GA), and differential evolution (DE) for optimizing the problem in Equation (10) [39]. In each generation 50 parent individuals formed the basis for creating a total of 105 children individuals by means of mutation (30), recombination (45), crossover (15), and the Montecarlo method (15). The optimization parameters used for children generation are listed in Table 5. Selection was carried out by means of the NSGA-II algorithm [46]. Optimization stopped after 1000 generations. Three similar optimization runs were carried out to address the stochastic nature of this optimization method. The individual analysis ran on 50 parallel processes on the high performance computing system of the Center for Information Services and High Performance Computing (ZIH), TU Dresden. Calculations were performed on Xeon Platinum 8470 processors at 2.0 GHz.

Table 5 – Optimization parameters for children generation in evolutionary algorithms. "#" stands for "number of".

method	parameter description	value
crossover (GA)	# crossover points	3
mutation (GA)	mutation probability	0.005
mutation (ES)	mutation strength	0.2
discrete recombination (ES)	# parents	2
	# children	2
global intermediate recombination (ES)	# parents	2
local intermediate recombination (ES)	# parents	2
mutation (DE)	mutation strength	0.5
	# difference vectors	2
recombination (DE)	crossover constant	0.5

3. Results

3.1 Design level 1: Layup

Non-linear structural analysis is supposed to allow bifurcation in the panel response due to shear loading. Figure 5 depicts this bifurcation in terms of a typical buckle propagation. At first, the structural response is dominated by the geometrically linear shear strain. After that, a first shear buckle gradually evolves. It follows the panel diagonal as it is expected due to the quadratic shape. With increased loading, the buckling shape is narrowing more and is pushed towards the panel corners.

Symmetric layups without ply repetition and balanced angles in y-direction were produced in design level 1 by means of the present optimization workflow. On the one hand, three QI layups were found by the optimizer with ply numbers n_l between 16 and 32. While all three layups showed invariant in-plane stiffnesses, fewer plies led to higher errors of rotational invariance of out-of-plane stiffnesses (cf. Table 6).

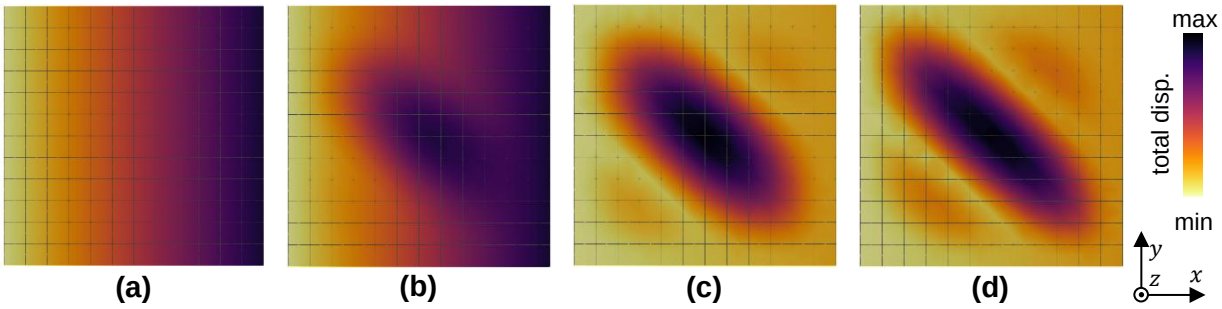


Figure 5 – Illustrative example of the typical shear buckle propagation (a) to (d) with increasing displacement s in load direction produced by means of non-linear structural analysis. Total displacement is first dominated by geometrically linear shear strain, finally by the global skin buckling (c), which moves further towards the panel corners (d).

Table 6 – Results of design level 1 for quasi-isotropic layups.

layup	n_l	$\lvert 1 - A_{22}/A_{11} \rvert$	$\lvert 1 - D_{22}/D_{11} \rvert$
$[0/-45/(90/45)_2/-45/45/0/-45/(0/90)_2/45/-45]_s$	32	0.00 %	0.32 %
$[90/45/(-45/0)_2/45/0/90/45/-45/90]_s$	24	0.00 %	3.90 %
$[-45/45/90/0/45/0/90/-45]_s$	16	0.00 %	8.73 %

On the other hand, anisotropic layups were optimized regarding the objective functions described in Equation (12). All results are displayed in Figure 6 in terms of the structural mass m and each of the structural performance quantities: buckling load F_B, buckling factor λ_B, and postbuckling stiffness K_{post}. QI layups and an aluminium reference with the same structural mass was added for comparison.

It appears plausible that the formulations O1, O2, and O3 excel in F_B, λ_B, and K_{post}, respectively, as they include these performance quantities are part of the objective function. The overall differences in F_B and λ_B between O1 to O4 remain small. Values for λ_B stay above 10 throughout all optimizations. Formulations O3 and O4 do not seem to have a different result domain, suggesting a strong weight for K_{post} in optimization. The QI layups are in the same range of formulations O1 to O4 for F_B and λ_B, but are falling behind for K_{post}. It is obvious that the aluminium panels show considerably lower F_B while approaching the same values for λ_B. Differences in K_{post} grow with larger structural masses regarding the objective function formulations O1, O3, and O4. Nevertheless, the aluminium panels exhibit less values for all performance quantities than the panels with QI layups.

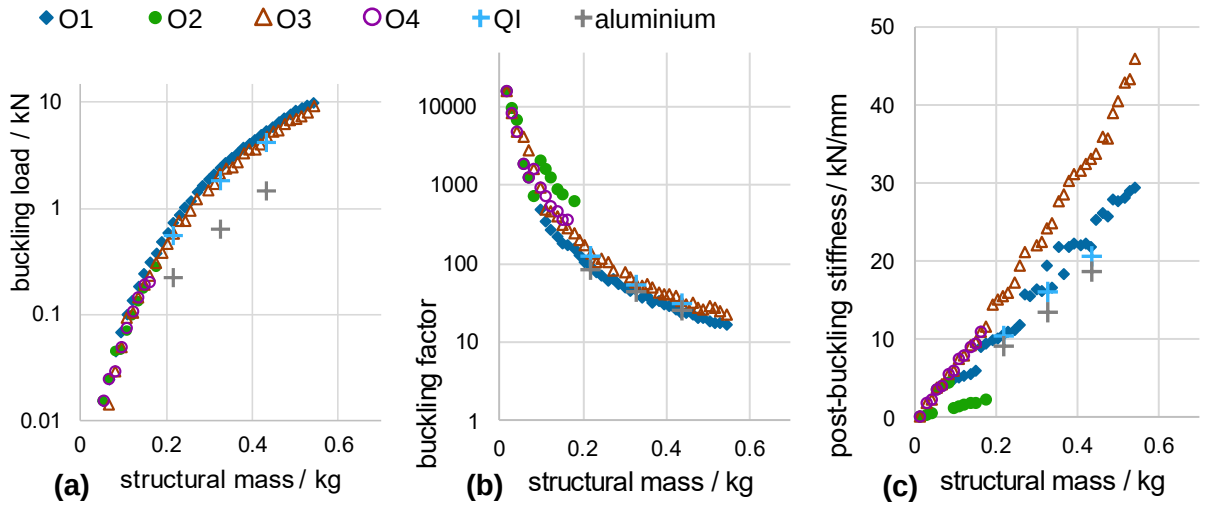


Figure 6 – Optimization results from design level 1 regarding structural mass, buckling load, buckling factor, and postbuckling stiffness: Objective function formulations O1 to O4 are displayed against quasi-isotropic (QI) laminates and the

aluminium reference.

3.2 Design level 2: Ideally stiffened plate

The QI layup with 24 plies from Table 6 is used throughout optimization of the objective function formulations O1 to O4, so that mainly stringer properties and positions determine the structural response. As for design level 1, Figure 7 depicts the optimization results in terms of the structural mass m as well as the structural performance quantities buckling load F_B, buckling factor λ_B, and postbuckling stiffness K_{post}. Structural solutions without stringers are excluded as they represent design level 1.

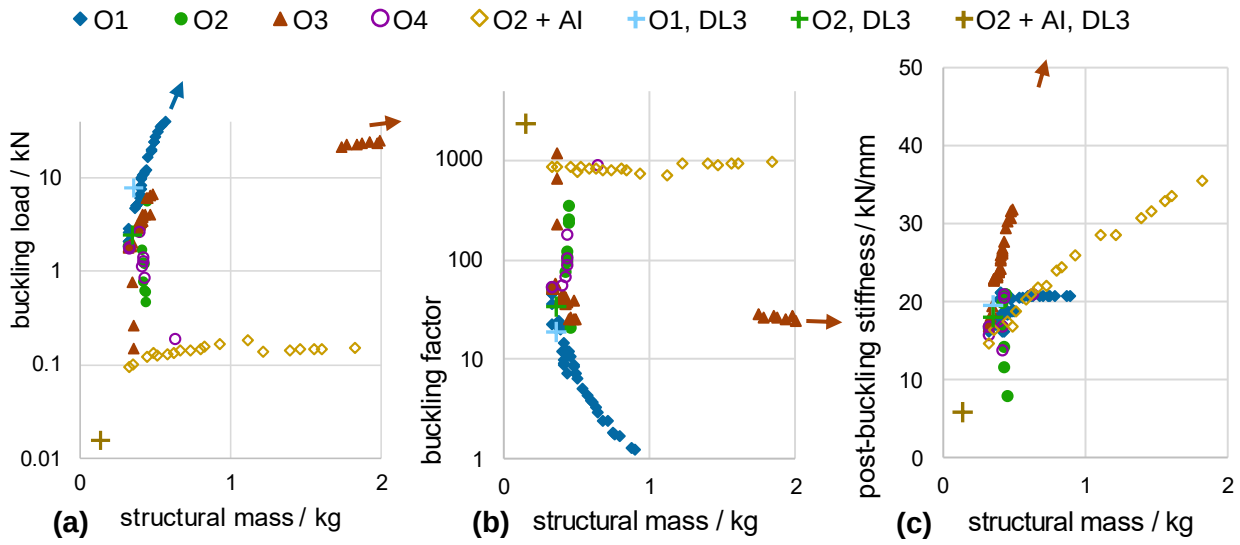


Figure 7 – Optimization results from design level 2 regarding structural mass, buckling load, buckling factor, and postbuckling stiffness: Optimization goals O1 to O4 as well as O2 with anisotropic (AI) layup optimization are displayed against derived detailed solutions for design level 3. Arrows indicate further solutions not shown in this figure.

Optimization results diverge between the objective function formulations especially for larger values of m. Values of F_B are 2 to 3 times higher than in design level 1 for formulation O1, while λ_B approach 1. Formulation O3 generated solutions with mass values over 2 kilograms not shown in the diagrams but indicated with arrows. Two solution groups are clearly separated, standing for two different stringer configurations. Again, formulation O4 exhibits a similar result domain as O2. However, a single solution here with slightly higher mass m aligns itself with the optimization formulation O2+AI, which stands for an additional optimization of anisotropic layups. The appropriate results incorporate thin laminates with 7 to 8 plies. Hence, the partial effects of skin and stringer stiffening are differently distributed for results of both formulations but yield the same overall stiffening effect. Results for O2+AI exhibit only a small range of structural performance over a large range for values for m, mainly contributed by the stringer stiffening.

3.3 Design level 3: Plate with stiffener debonding failure

Specific results from design level 2 served as a basis for the generation of detailed panel models in design level 3 according to Section 2.1. Bending area moments of the generic stringer properties of design level 2 were sufficiently met (cf. Table 7). However, torsional area moments are significantly underestimated compared to the optimized parameters. This discrepancy stems from the particular shape of Z-stringer cross-section which cannot scale values of I_t sufficiently independently of $I_{\eta\eta}$ or I_{zz}, as it was, however, assumed by the optimization problem.

Table 7 – Accuracy of stringer modelling in design level 3.

parameter	individual O1	individual O2	individual O2 + AI
length of stringer flange / mm	10.0	10.0	10.0
length of stringer web / mm	7.6	5.0	24.0
length of stringer cap / mm	8.0	20.7	22.6
rel. error $I_{\eta\eta}$	+0.11 %	+1.22 %	+0.38 %
rel. error I_{zz}	-0.38 %	-0.55 %	+0.12 %
rel. error I_t	+99.8 %	+97.0 %	+99.4 %

Furthermore, stringer lines in design level 2 with small distances in between can only be transferred to detailed stringer models by combining the properties to a single stringer. All these inherent uncertainties led to remarkable differences in the structural response between the two design levels, which are listed in Table 8. The failure load F_f drops less than the buckling load F_B so that a higher buckling factor λ_B is achieved in design level 3. A lower F_B may be related to the much lower torsional area moment of the detailed stringer model. A larger postbuckling stiffness K_{post} for the detailed panel may be attributed to a larger contact area between stringers and skin, that influences the forming of postbuckling shapes. Last, a considerably lower mass in design level 3 is expected because values of the structural mass m are only upper bounds in design level 2 due to an assumed adverse cross-sectional shape of the stringers, as described via Equations (1) to (4).

A comparison of the postbuckling shapes for all structural solutions of both design levels is shown in Figure 8. Same load factors related to the first buckling load F_B are applied. The general buckle positions are similar with a lower displacement amplitude in z-direction, s_z, for results of design level 3, caused by lower buckling loads F_B.

Table 8 – Comparison of performance measures for structural solutions of design level 2 and 3.

individual		m / kg	F_B / kN	λ_B	F_f / kN	K_{post} / kN/mm
O1	design level 2	0.448	16.2	10.4	168	18.4
	design level 3	0.353	7.79	18.6	145	19.5
	error	-21.2 %	-52.0 %	+79.9 %	-13.6 %	+6.2 %
O2	design level 2	0.447	5.47	20.5	112	14.1
	design level 3	0.347	2.46	33.1	81.3	17.9
	error	-22.4 %	-55.1 %	+61.7 %	-27.4 %	+26.7 %
O2 + AI	design level 2	0.445	0.121	848	102	17.5
	design level 3	0.136	0.0154	2340	35.9	5.75
	error	-69.4 %	-87.3 %	+176 %	-64.9 %	-67.2 %

Figure 9 illustrates the failure index for a detailed panel model. Particularly, the stringer tails are likely to fail first at the bonding interface. Critical regions are those which are distorted by the postbuckling shape of the skin. A detail view reveals that also the stringer web is considerably stressed there.

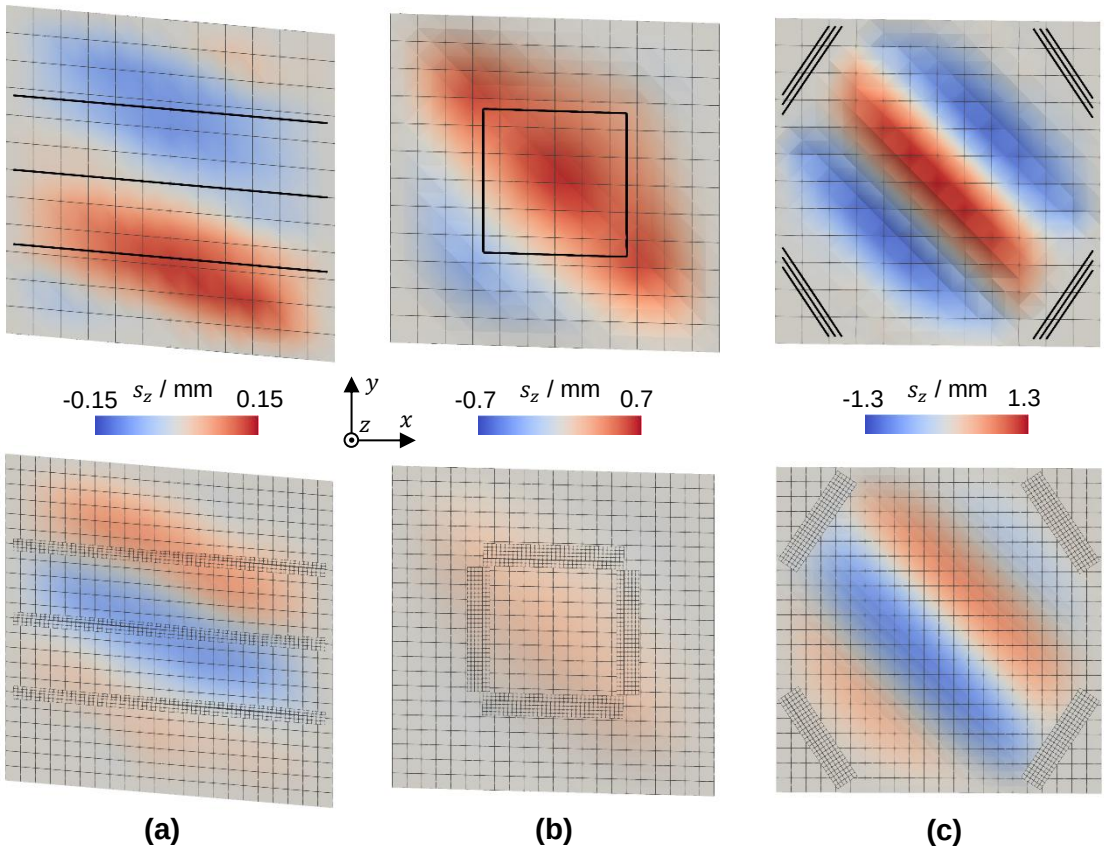


Figure 8 – Comparison of buckling shapes between design levels 2 and 3 with the same load factor relative to the buckling load: (a) Solution for O1 with factor 1.00. (b) Solution for O2 with factor 1.01. (c) Solution for O2 and anisotropic layup optimization with factor 36.4.

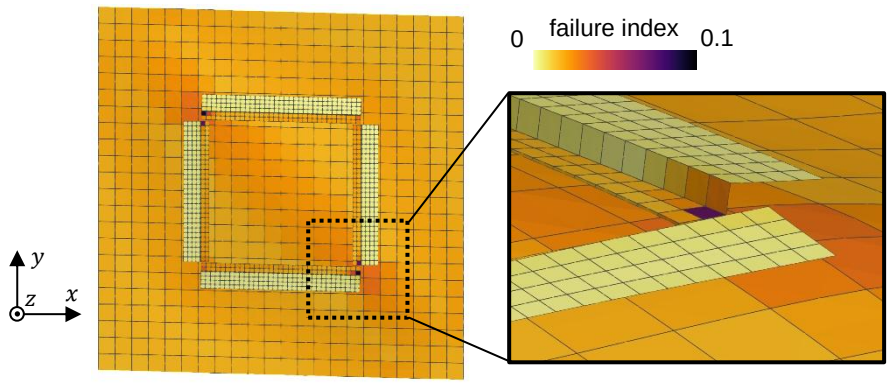


Figure 9 – Failure index of a solution for O2 at design level 3: Detail image is showing a larger failure index at the stringer tails with highly loaded stringer flange and medium loaded stringer web.

4. Discussion

4.1 Different objective functions

Structural results generated by the panel optimization depend on the appropriate objective function, especially for the stiffened panel in design levels 2 and 3. This means that the solution range should be carefully adjusted via a specific formulation of the optimization problem. While general solutions such as QI laminates are designed for a rather robust structural response, specific optimization goals such as a maximum buckling load or a high buckling factor may induce inferior performance in terms of another property. Optimization results in this study suggest the buckling load F_B and the postbuckling stiffness K_{post} can be effectively maximized in order to delay first buckling and to

achieve high structural stiffnesses, respectively, even in the postbuckling regime.

Design level 1 incorporates a quite narrow result domain which leads to the assumption that even for thin-ply material the design space is too small for a more specific structural performance, e.g., a specifically high buckling load. To this end, QI laminates reach similar values of structural response despite the generic objective. This study shows at the same time consistently inferior results for unstiffened aluminium panels, which indicates the overall advantage of using CFRP for this present structural design task.

This image changes with the introduction of stringer stiffening: Results exhibit considerably larger variation for different objective functions. Consequently, the larger design space, now including stringer positions and cross-sectional properties, is necessary for a distinctive structural design. With the additional optimization of the skin layup, results only comprise a limited range. This suggests contrariwise a too large design space for the optimization problem setup in the present study. It is likely that, e.g., more individuals or a longer optimization run with more than 1000 generations will yield a larger result domain. This would lead to even more computational resources needed for optimization than in this study (cf. Table 9). Investigations would then be needed to find a more efficient optimization method, e.g., partially based on gradient methods. Against this background, a stepwise approach proposed in this study seems generally useful for the design of stiffened shell structures for a computationally efficient optimization procedure.

Table 9 – Comparison of optimization wall clock and CPU times for different design levels 2 and 3 and 50 parallel processes.

optimization	total wall clock time	total CPU time	CPU time per generation
design level 2	~26 h	~55 d	~1:20 h
design level 3	~37 h	~77 d	~1:50 h

Both design levels 1 and 2 feature very high buckling factors λ_B of about 10 to 30 for a structural mass of $m \approx 0.5\,\mathrm{kg}$. However, results vary largely, especially for objective function formulation O2 that particularly aims at maximum values of λ_B. This may be caused by both the variation of the buckling load F_B as well as the estimated failure load F_f. In most of the non-linear structural analyses carried out in the present study via b2000++pro, no convergence until the maximum load value $F_{\max}$ of Equation (7) is achieved. With complex structural configurations including skin and stringers, a robust F-s curve analysis seems essential. Better comparable results may also be achieved by maximizing the failure load F_f instead of the buckling factor λ_B as a compound quantity. Nevertheless, more detailed models of design level 3 suggest that values for λ_B clearly beyond the common value of 1.5 seem generally achievable. Numerical investigations with a more precise failure criterion or a highly detailed FE model for validation are still needed in future.

4.2 Viability of modelling approach

Structural optimization requires FE models with a sufficiently low level of details to limit the required computational resources. Therefore, approximations in the structural response may lead to imprecise structural behaviour in general and even to insufficient convergence, as raised in Section 4.1. The stringer approximation via line geometries in design level 2 then needs to be transferred to more detailed FE models in design level 3, which also holds uncertainties. These are specified in Table 7 in terms of the stringer cross-sectional properties and in Table 8 for the overall structural response. Some of these uncertainties may be reduced by imposing the appropriate optimization constraints, like a minimum stringer distance from each other and sufficient stringer tail clearance. Also, a proper design space for the torsional area moment I_t should be defined according to the shape of the stringer cross-section, presumably even dependent on the bending area moments $I_{\eta\eta}$

and I_{zz}. With it, a more precise first buckling load F_B could be determined also for the detailed models of design level 3.

The shear panel only incorporates one load direction in the present study. Although layups were optimized with angles balanced in y-direction, different structural responses are assumed for different load signs. On the one hand, two different load cases could be investigated in further optimization studies. On the other hand, extensive post-processing is viable by means of result variations, e.g., in the sequence of ±45° plies.

Furthermore, the modelling of debonding failure is crucial for a precise prediction of the failure load. This requires the detailed knowledge of the cohesive zone properties including damage mechanisms. In the present study only linear-elastic material is considered. Hence, no non-linear material effects such as the plasticity behaviour can be reproduced by the FE models here. However, first failure analysis by means of only material strength values already permit the assessment of the yield point as a conservative failure prediction. Experimental validation studies are needed in the future to strengthen these findings.

5. Conclusion and outlook

This study presents a stepwise approach for the design of stiffened shell structures. In design levels 1 and 2, the skin layup and stringer configuration of the structure are separately optimized and proposed for a more detailed modelling in design level 3. Stringer cross-sections in design level 2 only hold generic properties in terms of the area moments, where design level 3 incorporate concrete cross-sectional shapes. Results suggest that a stepwise approach is useful to reduce the computational effort of structural optimization.

Specific optimization function formulations lead to distinctive structural performance. Additional stringers in design level 2 clearly amplify this effect compared to design level 1. It has been revealed that the optimization of the buckling factor exhibits large result variations over a small range of structural mass. Therefore, using the failure load as an objective is suggested instead.

Even for detailed models in design level 3, high buckling factors of over 10 are reached for a structural mass of about 0.5 kilograms. Hence, the present optimization approach may be straightforwardly applied to the postbuckling design of lightweight shear-loaded helicopter shell structures. Optimized structures with thermoplastic CFRP material exhibit better performance in terms of buckling load, buckling factor, and postbuckling stiffness than their aluminium counterparts. This holds even for QI layups as a generic robust design solution based on CFRP material.

Analysis of the failure index in design level 3 identify the stringer tails close to high buckling-induced skin curvature as the most critically stressed structural parts. Non-linear material models including plasticity and damage mechanisms are needed for future detailed investigations.

There are limitations in transferring simple structural models of the stiffened panel in design level 2 to more detailed models in design level 3 regarding, e.g., a minimum stringer distance or a sufficient stringer tail clearance. Numerical and experimental studies are needed for further validation of the viability of the modelling approach.

Acknowledgements

The authors gratefully acknowledge the project funding by the Federal Ministry for Economic Affairs and Energy (BMWE), Germany, grant no. 20W2208D, enabled by resolution of the German Bundestag. This work was conducted within the NATURE consortium. Moreover, the authors would like to thank the German Aerospace Center (DLR) for providing the FE solver b2000++pro as part of the joint development. They further gratefully acknowledge the NHR Center of TU Dresden, Germany, who made available computing time to them on the high-performance computer. This center is jointly supported by the Federal Ministry of Education and Research (BMBF), Germany, and the state governments participating in the NHR (www.nhr-verein.de/unsere-partner).

Copyright statement

The authors confirm that they, and/or their company or organization, hold copyright on all of the original material included in this paper. The authors also confirm that they have obtained permission, from the copyright holder of any third party material included in this paper, to publish it as part of their paper. The authors confirm that they give permission, or have obtained permission from the copyright holder of this paper, for the publication and distribution of this paper as part of the ICAS proceedings or as individual off-prints from the proceedings.

References

[1] KASSAPOGLOU, C.: *Design and Analysis of Composite Structures: With Applications to Aerospace Structures*. Second ed. West Sussex, United Kingdom: John Wiley & Sons, Ltd, 2013 (Aerospace series). – ISBN 9780470972700

[2] JANEK, M.; GÖRICK, D.; LARSEN, L.; JARKA, S.; KUPKE, M.: Investigation of power and amplitude control in continuous ultrasonic welding of unidirectional CFRPs: A comparative study. In: *Composites Part A: Applied Science and Manufacturing* 199 (2025), p. 109194. doi:10.1016/j.compositesa.2025.109194. – ISSN 1359–835X

[3] RAPS, L.; CHADWICK, A. R.; VOGGENREITER, H. F.: Steering for in-situ AFP-manufactured structures: Part 1 - Critical arc length. In: *Composite Structures* 381 (2026), p. 120023. doi:10.1016/j.compstruct.2025.120023. – ISSN 0263–8223

[4] RAPS, L.; CHADWICK, A. R.; SCHÄFER, Y.; VOGGENREITER, H. F.: Steering for in-situ AFP-manufactured structures: Part 2 - Optimized layup strategy. In: *Composite Structures* 381 (2026), p. 120024. doi:10.1016/j.compstruct.2025.120024. – ISSN 0263–8223

[5] KRUEGER, R.; BERGAN, A.: Advances in Thermoplastic Composites Over Three Decades – A Literature Review. 2024 (20240005376). https://ntrs.nasa.gov/citations/20240005376

[6] GALOS, J.: Thin-ply composite laminates: a review. In: *Composite Structures* 236 (2020), p. 111920. doi:10.1016/j.compstruct.2020.111920. – ISSN 0263–8223

[7] ARTEIRO, A.; FURTADO, C.; CATALANOTTI, G.; LINDE, P.; CAMANHO, P.: Thin-ply polymer composite materials: A review. In: *Composites Part A: Applied Science and Manufacturing* 132 (2020), p. 105777. doi:10.1016/j.compositesa.2020.105777

[8] FURTADO, C.; ARTEIRO, A.; CATALANOTTI, G.; XAVIER, J.; CAMANHO, P.: Selective ply-level hybridisation for improved notched response of composite laminates. In: *Composite Structures* 145 (2016), p. 1–14. doi:10.1016/j.compstruct.2016.02.050

[9] HO, Y.-C.; SASAYAMA, H.; YANAGIMOTO, J.: Mechanical properties and drawing process of multilayer carbon-fiber-reinforced plastic sheets with various prepreg thicknesses. In: *Advances in Mechanical Engineering* 9 (2017), No. 3, p. 168781401769269. doi:10.1177/1687814017692695

[10] GARCÍA-RODRÍGUEZ, S.; COSTA, J.; BARDERA, A.; SINGERY, V.; TRIAS, D.: A 3D tomographic investigation to elucidate the low-velocity impact resistance, tolerance and damage sequence of thin non-crimp fabric laminates: effect of ply-thickness. In: *Composites Part A: Applied Science and Manufacturing* 113 (2018), p. 53–65. doi:10.1016/j.compositesa.2018.07.013

[11] GUILLAMET BUSQUETS, G.: *Improved delamination resistance of thin-ply based laminates: an experimental and numerical study*, Universitat de Girona, Dissertation, July 2016. http://www.tdx.cat/-handle/10803/387822

[12] MARKATOS, D. N.; PANTELAKIS, S. G.: Assessment of the Impact of Material Selection on Aviation Sustainability, from a Circular Economy Perspective. In: *Aerospace* 9 (2022), No. 2, p. 52. doi:10.3390/aerospace9020052

[13] FINK, A.; KEMPF, M.; BEIER, U.: A structural panel with carbon composite plies (EP4685048A1) /

European Patent Office. 2026. https://worldwide.espacenet.com/patent/search/family/091967133/-publication/EP4685048A1

[14] ZIMMERMANN, R.; KLEIN, H.; KLING, A.: Buckling and postbuckling of stringer stiffened fibre composite curved panels – Tests and computations. In: *Composite Structures* 73 (2006), No. 2, p. 150–161. doi:10.1016/j.compstruct.2005.11.050. – ISSN 0263–8223

[15] BISAGNI, C.: *Buckling and postbuckling structures – experimental, analytical and numerical studies*. *Chapter* Buckling and Postbuckling Tests on Stiffened Composite Panels and Shells. London: Imperial College Press, 2008. – ISBN 1860947948, p. 39–64

[16] DEGENHARDT, R.; KLING, A.; ROHWER, K.; ORIFICI, A.; THOMSON, R.: Design and analysis of stiffened composite panels including post-buckling and collapse. In: *Computers & Structures* 86 (2008), No. 9, p. 919–929. doi:10.1016/j.compstruc.2007.04.022

[17] KLING, A.: *Buckling and postbuckling structures – experimental, analytical and numerical studies*. *Chapter* Stability Design of Stiffened Composite Panels – Simulation and Experimental Validation. London: Imperial College Press, 2008. – ISBN 1860947948, p. 141–176

[18] BERTOLINI, J.; CASTANIÉ, B.; BARRAU, J.-J.; NAVARRO, J.-P.: An experimental and numerical study on omega stringer debonding. In: *Composite Structures* 86 (2008), No. 1-3, p. 233 – 242

[19] YAP, J. W.; THOMSEN, R. S.; SCOTT, M. L.; HACHENBERG, D.: Influence of post-buckling behavior of composite stiffened panels on the damage criticality. In: *Composite Structures* 66 (2004), p. 197–206

[20] BISAGNI, C.; DÁVILA, C. G.: Experimental investigation of the postbuckling response and collapse of a single-stringer specimen. In: *Composite Structures* 108 (2014), p. 493–503. doi:10.1016/j.compstruct.2013.09.018

[21] ZHAO, L.; WANG, K.; DING, F.; QIN, T.; XU, J.; LIU, F.; ZHANG, J.: A post-buckling compressive failure analysis framework for composite stiffened panels considering intra-, inter-laminar damage and stiffener debonding. In: *Results in Physics* 13 (2019), p. 102205. doi:10.1016/j.rinp.2019.102205

[22] CUNHA, F. R. S.; WILLE, T.; DEGENHARDT, R.; SINAPIUS, M.; ARAÚJO, F. C.; ZIMMERMANN, R.: A robustness-based design strategy for composite structures. In: *Aircraft Engineering and Aerospace Technology* 86 (2014), No. 4, p. 274–286. doi:10.1108/aeat-04-2013-0070

[23] CUNHA, F. R. S.; WILLE, T.; DEGENHARDT, R.; SINAPIUS, M.; ARAÚJO, F. C.; ZIMMERMANN, R.: A robustness-based design strategy for composite structures probabilistic approach. In: *Aircraft Engineering and Aerospace Technology* 86 (2014), No. 4, p. 262–273. doi:10.1108/aeat-04-2013-0071

[24] FAGGIANI, A.; FALZON, B. G.: Optimization Strategy for Minimizing Damage in Postbuckling Stiffened Panels. In: *AIAA Journal* 45 (2007), No. 10, p. 2520. doi:10.2514/1.26910

[25] LIANG, K.; LI, Z.: Postbuckling analysis and optimization of composite laminated panels using a novel perturbation-based approximation FE method. In: *Thin-Walled Structures* 160 (2021), p. 107398. doi:10.1016/j.tws.2020.107398. – ISSN 0263–8231

[26] GRENESTEDT, J. L.: Layup optimization against buckling of shear panels. In: *Structural Optimization* 3 (1991), No. 2, p. 115–120. doi:10.1007/bf01743281. – ISSN 1615–1488

[27] VITALI, R.; PARK, O.; HAFTKA, R. T.; SANKAR, B. V.; ROSE, C. A.: Structural Optimization of a Hat-Stiffened Panel Using Response Surfaces. In: *Journal of Aircraft* 39 (2002), No. 1, p. 158–166. doi:10.2514/2.2910. – ISSN 1533–3868

[28] HENRICHSEN, S. R.; WEAVER, P. M.; LINDGAARD, E.; LUND, E.: Post-buckling optimization of composite structures using Koiter's method. In: *International Journal for Numerical Methods in Engineering* 108 (2016), No. 8, p. 902–940. doi:10.1002/nme.5239. – ISSN 1097–0207

[29] NI, X.-Y.; PRUSTY, B. G.; HELLIER, A. K.: Buckling and post-buckling of isotropic and composite stiffened panels: a review on optimisation (2000-2015). In: *International Journal of Maritime Engineering* 158 (2016), No. A3. doi:10.3940/rina.ijme.2016.a3.388

[30] HAFTKA, R. T.; WALSH, J. L.: Stacking-sequence optimization for buckling of laminated plates by integer programming. In: *AIAA Journal* 30 (1992), No. 3, p. 814–819. doi:10.2514/3.10989. – ISSN 1533–385X

[31] NAGENDRA, S.; JESTIN, D.; GÜRDAL, Z.; HAFTKA, R.; WATSON, L.: Improved genetic algorithm for the design of stiffened composite panels. In: *Computers & Structures* 58 (1996), No. 3, p. 543–555. doi:10.1016/0045-7949(95)00160-i. – ISSN 0045–7949

[32] BRUYNEEL, M.: Optimization of laminated composite structures: problems, solution procedures and applications. In: *Composite Materials Research Progress* (2008). https://orbi.uliege.be/bitstream/2268/-184951/1/Bruyneel_A4.pdf

[33] CHU, S.; FEATHERSTON, C.; KIM, H. A.: Design of stiffened panels for stress and buckling via topology optimization. In: *Structural and Multidisciplinary Optimization* 64 (2021), No. 5, p. 3123–3146. doi:10.1007/s00158-021-03062-3. – ISSN 1615–1488

[34] PARADIES, R.: Designing quasi-isotropic laminates with respect to bending. In: *Composites Science and Technology* 56 (1996), No. 4, p. 461–472. doi:10.1016/0266-3538(96)00006-1. – ISSN 0266–3538

[35] GRÉDIAC, M.: A Procedure for Designing Laminated Plates with Required Stiffness Properties. Application to Thin Quasi-Isotropic Quasi-Homogeneous Uncoupled Laminates. In: *Journal of Composite Materials* 33 (1999), No. 20, p. 1939–1956. doi:10.1177/002199839903302005. – ISSN

1530–793X

[36] VANNUCCI, P.: The Design of Laminates as a Global Optimization Problem. In: *Journal of Optimization Theory and Applications* 157 (2012), No. 2, p. 299–323. doi:10.1007/s10957-012-0175-6. – ISSN 1573–2878

[37] QU, S.; KENNEDY, D.; FEATHERSTON, C. A.: A multilevel framework for optimization of an aircraft wing incorporating postbuckling effects. In: *Proceedings of the Institution of Mechanical Engineers, Part G: Journal of Aerospace Engineering* 226 (2011), No. 7, p. 830–845. doi:10.1177/0954410011415158

[38] MAUERSBERGER, M.; HAUFFE, A.; HÄHNEL, F.; DEXL, F.; MARKMILLER, J. F. C.: Topology optimization of a benchmark artifact with target stress states using evolutionary algorithms. In: *Engineering with Computers* 40 (2023), No. 2, p. 1265–1288. doi:10.1007/s00366-023-01860-5. – ISSN 1435–5663

[39] SEEGER, J.; WOLF, K.: Multi-objective design of complex aircraft structures using evolutionary algorithms. In: *Proceedings of the Institution of Mechanical Engineers, Part G: Journal of Aerospace Engineering* 225 (2011), No. 10, p. 1153–1164. doi:10.1177/0954410011411384. – ISSN 0954–4100, 2041–3025

[40] DEXL, F.; HAUFFE, A.; WOLF, K.: Comparison of structural parameterization methods for the multidisciplinary optimization of active morphing wing sections. In: *Computers & Structures* 263 (2022), p. 106743. doi:10.1016/j.compstruc.2022.106743. – ISSN 0045–7949

[41] SMR ENGINEERING & DEVELOPMENT: Post-buckling Analysis of Composite Panels – Towards Fast Tools with Implicit FEM Methods. In: *Fifth Community Aeronautical Days – Aeronautics Days 2006*, 2006, https://www.smr.ch/projects/cocomat-aerodays-2006.pdf

[42] RAPS, L.; CHADWICK, A.; SCHIEL, I.; SCHMIDT, I.: CF/LM-PAEK: Characterisation and sensitivity to critical process parameters for automated fibre placement. In: *Composite Structures* 284 (2022), p. 115087. doi:10.1016/j.compstruct.2021.115087. – ISSN 0263–8223

[43] HASHIN, Z.: Failure Criteria for Unidirectional Fiber Composites. In: *Journal of Applied Mechanics* 47 (1980), No. 2, p. 329. doi:10.1115/1.3153664. – ISSN 00218936

[44] REDDY, J. N.: *Mechanics of laminated composite plates and shells: theory and analysis*. 2nd ed. Boca Raton: CRC Press, 2004. – 831 p. http://www.loc.gov/catdir/enhancements/fy0646/2003061067-d.html. – ISBN 978–0–8493–1592–3

[45] MARTINS, J. R. R. A.; NING, A.: *Engineering Design Optimization*. Cambridge University Press, 2021. doi:10.1017/9781108980647. – ISBN 9781108833417

[46] DEB, K.; PRATAP, A.; AGARWAL, S.; MEYARIVAN, T.: A fast and elitist multiobjective genetic algorithm: NSGA-II. In: *IEEE Transactions on Evolutionary Computation* 6 (2002), No. 2, p. 182–197. doi:10.1109/4235.996017